

RSC Advances



This is an *Accepted Manuscript*, which has been through the Royal Society of Chemistry peer review process and has been accepted for publication.

Accepted Manuscripts are published online shortly after acceptance, before technical editing, formatting and proof reading. Using this free service, authors can make their results available to the community, in citable form, before we publish the edited article. This *Accepted Manuscript* will be replaced by the edited, formatted and paginated article as soon as this is available.

You can find more information about *Accepted Manuscripts* in the [Information for Authors](#).

Please note that technical editing may introduce minor changes to the text and/or graphics, which may alter content. The journal's standard [Terms & Conditions](#) and the [Ethical guidelines](#) still apply. In no event shall the Royal Society of Chemistry be held responsible for any errors or omissions in this *Accepted Manuscript* or any consequences arising from the use of any information it contains.

1 **Magnetized property effect of a non-aqueous solvent upon complex**
2 **formation between kryptofix 22DD with lanthanum (III) cation:**
3 **experimental aspects and molecular dynamics simulation**
4

5 *Gholam Hossien Rounaghi¹, Mostafa Gholizadeh, Fatemeh Moosavi, Iman Razavipanah, Hossein Azizi-*
6 *Toupkanloo, and Mohammad Reza Salavati*

7
8 **Abstract**

9 The complexation reaction between La^{3+} cation and the macrocyclic ligand (kryptofix 22DD)
10 in ordinary methanol (MeOH) and extraordinary methanol solvent (magnetized methanol)
11 exposed in a magnetic field at different temperatures has been investigated using the
12 conductometric method, in order to determine the effect of magnetic solvents on the
13 thermodynamics of the complexation process between the metal cation and the ligand. The
14 stoichiometry of the complex formed between La^{3+} cation and the ligand is 1:1 [M:L] in both
15 solvent systems. Comparison of the corresponding molar conductivity versus $[\text{L}]_t/[\text{M}]_t$ for
16 (kryptofix 22DD.La)³⁺ complex shows that the complex formed between the metal cation and
17 kryptofix 22DD in the magnetized methanol is weaker compared to the ordinary methanol. The
18 result of the density functional theory clears that addition of the metal ion to the ligand,
19 completely deforms the ligand from its planar shape and the orientation of two carbon chains
20 attached to the ring, changes in comparison with the free ligand. In addition, the molecular

Gholam Hossein Rounaghi (✉)•Mostafa Gholizadeh•Fatemeh Moosavi•Iman Razavipanah•Mohammad Reza Salavati

Department of Chemistry, Faculty of Sciences, Ferdowsi University of Mashhad, Mashhad, Iran

E-mail address: ghrounaghi@yahoo.com and ronaghi@um.ac.ir

Tel: 0098- 51-37626388

Fax: 0098- 51- 38796416

Hossein Azizi-Toupkanloo

Department of Chemistry, Faculty of Sciences, University of Neyshabur, Neyshabur, Iran

21 dynamics simulation can shed light on the influence of the magnetic field, from the molecular
22 point of view, on the properties of solvents and is able to explain the variation of hydrogen bond
23 and transport properties. These changes may be the reason for the interaction of the solvent and
24 the solute, as well as, the stability constant of the complex formed between La^{3+} cation and
25 kryptofix 22DD in solutions. As the strength of the magnetic field increases, the number of the
26 hydrogen bonds formed between the methanol molecules increases and the methanol self-
27 diffusion coefficient decreases. These changes restrict the movement of the molecules which
28 results in increasing the viscosity of the methanol and therefore, the stability constant of the
29 (kryptofix 22DD.La) $^{3+}$ complex decreases in magnetized methanol with respect to the ordinary
30 methanol.

31

32 **Keywords:** Complexation● Kryptofix 22DD● Lanthanum(III) cation● Magnetized methanol●
33 Density functional theory● Molecular dynamics simulation● Self-diffusion coefficient

34

35 **Introduction**

36 The cryptand compounds, which are used in many fascinating areas of chemistry,
37 biochemistry, and material science,¹⁻⁵ were first synthesized by Lehn et al.⁶ They are
38 macrobicyclic ligands that contain an internal cavity of about spherical shape well suited for the
39 recognition of the spherical cations.⁷ Cryptands form very stable and selective complexes with a
40 variety of metal cations.^{7,8} Their alkali ion complexes possess stabilities several orders of
41 magnitude higher than natural or synthetic macrocyclic ligands,³ a phenomena which is called
42 the “cryptate effect”.⁹

43 Lanthanides are widely distributed in low concentrations throughout the Earth's crust.¹⁰ La³⁺
44 cation with potentially high and variable coordination numbers and flexible coordination
45 environments behaves as a hard acid with a strong affinity for a hard base containing neutral and
46 negatively charged oxygen atoms.¹¹⁻¹⁵

47 In solutions, the metal ion, the macrocyclic ligand, and also the metal ion-macrocyclic ligand
48 complex would be surrounded by the solvent molecules. Because of having different
49 physicochemical properties, each solvent can effect on the stability of metal ion complexes in
50 different ways. Therefore, it is of great importance to study the effect of solvent on the
51 complexation of metal ions with the macrocyclic ligands. One approach to achieve a detailed
52 understanding of these interactions is to study the influence of magnetic field on the
53 physicochemical properties of solvent and as a consequence on the formation of metal ion-
54 macrocyclic complexes in solutions.

55 As the macrocyclic compounds are good models for the antibiotics and some of the other
56 drugs treatment in biological systems,¹⁶ it is of great interest to investigate the effect of magnetic
57 field upon complexation of such ligands with the metal ions. To our knowledge, the data about
58 the effect of magnetic field upon formation of metal ion-macrocyclic complexes in non-aqueous
59 solvents are very sparse. The first goal of the present study is to investigate how the magnetic
60 field can influence on the physicochemical properties of a non-aqueous solvent passing through a
61 magnetic field and as a result, the stability of the metal-ion complex at different temperatures.

62 The changes occurring in the structure of solvent under the effect of an external magnetic
63 field are important in various applications such as chemical processes. It has been found that
64 various aspects of the most common solvent (water) properties, including the size of the
65 cluster,¹⁷⁻¹⁹ hydrogen bonding,^{20, 21} electrical conductivity,²² dissolution rate into water,^{23, 24} van

66 der Waals bonding between molecules,²⁵ and its melting point²¹ change when it is exposed to a
67 magnetic field. Special attention has been devoted towards the the structure of alloy clusters²⁶ as
68 well as their growth.²⁷ Attempts to generate perpendicular magnetic anisotropy have been
69 performed to check the shape anisotropy due to dipolar interactions, experimentally and
70 theoretically. In addition, the use of a magnetic field is of considerable interest in a number of
71 practical applications due to the self-diffusion coefficient alteration under a magnetic field. From
72 molecular point of view, temperature influences on the properties of organic solvents in the
73 presence of a magnetic field, the point that has not yet been under investigation.

74 Molecular dynamics (MD) simulations provide a powerful means of investigating the
75 enhanced hydrogen bonding mechanism from an atomic viewpoint. Moreover, it is able to
76 explore how surrounded ions by the solvent molecules may be retarded providing complex. In
77 other words, solvent can effect on metal ion complex stability; as a result, achieving detailed
78 insight on the influence of magnetic field on the physicochemical properties of solvent is of great
79 importance. Temperature effect of external magnetic field on the properties of organic solvents
80 has not yet been reported. Therefore, the temperature effect on external magnetic field change
81 with the properties of methanol solvent is also under consideration to answer the above points in
82 line with experimental results.

83

84 **Experimental**

85 *Reagents and apparatus*

86 $\text{La}(\text{NO}_3)_3 \cdot 6\text{H}_2\text{O}$, 4,13-didecyl-1,7,10,16-tetraoxa-4,13-diazacyclooctadecane (kryptofix
87 22DD) and methanol with the highest purity were purchased from Merck (>99 % purity) and
88 were used without any further purification. The conductivity of methanol solvent was less than

89 $3.0 \times 10^{-7} \text{ S}^{-1} \text{ cm}^{-1}$ at 298.15 K. The conductance measurements were performed using a digital
90 Jenway conductometer (model 4510), in a water bath thermostated at a constant temperature
91 maintained within $\pm 0.1 \text{ }^\circ\text{C}$. The electrolytic conductance was measured using a dip-type
92 conductivity cell consisting of two platinum electrodes to which an alternating potential was
93 applied. A conductometric cell with a cell constant of 0.98 cm^{-1} was used throughout the study.

94 The static magnetic field in a compact form, a unit called "AQUA CORRECT", was used.
95 The equipment has a coaxial static magnetic system of 6000 G field strength, and was imported
96 from Germany (H.P.S Co.) [DN = 20, 3/4 in., flow $2 \text{ m}^3/\text{h}$] for the experiments. The equipment
97 was connected from one end to the liquid pump and the other end to the pipelines of the solvent
98 reservoir. The solvent had to flow through a coaxial static magnetic gap and came back to the
99 solvent reservoir. Therefore, the solvent could pass through the magnetic field for many times in
100 a closed cycle.

101 *Procedure*

102 The experimental procedure to obtain the stability constant of (kryptofix 22DD.La)³⁺ complex
103 by conductometric method in both ordinary and magnetized methanol solutions were as follows:
104 a solution of metal salt ($1.0 \times 10^{-4} \text{ M}$) was placed in a titration cell, thermostated at a given
105 temperature, and the conductance of the solution was measured. The ligand solution (2.0×10^{-3}
106 M) was transferred stepwise to the titration cell using a precalibrated microburette and the
107 conductance of the solution was measured after each transfer at the desired temperature. Adding
108 the ligand solution was continued until the total concentration of the kryptofix 22DD was
109 approximately five times higher than that of the metal cation. The conductance of the solution
110 was measured after each addition and the stability constant of the complex was obtained from
111 variation of molar conductance as a function of $[\text{L}]_t/[\text{M}]_t$ molar ratio plots using a GENPLOT

112 computer program.²⁸ This procedure was exactly carried out for the magnetized methanol
 113 solvent. The magnetized solvent was immediately used after passing through the magnetic field
 114 for 2 min.

115

116 Simulation details

117 Density functional theory (DFT) is known to handle geometries and vibrational frequencies
 118 of different systems especially hydrogen bonded systems appropriately accurate.²⁹⁻³¹ DFT
 119 method at B3LYP functional coupled with 6-311++G(d,p) basis set was employed, by using
 120 GAUSSIAN 03 package,³² to find the structural parameters for the ground state of target solvent
 121 and no restrictions on symmetries were imposed on the initial structure of the solvent. A
 122 vibrational analysis was performed to ensure the absence of negative vibrational frequencies and
 123 authenticate the existence of a true minimum.^{30,31} The geometrical parameters including bond
 124 lengths, bond angles, and dihedral angles, computed at B3LYP/6-311++G(d,p) level of theory as
 125 well as natural bond atomic charges were implemented in order to construct the initial
 126 configuration. In addition, for the description of the potential model, a classical force field
 127 approach has been used. The parametrized DREIDING force field applied to the MD
 128 simulations³³ has the following terms:

$$\begin{aligned}
 V_{\text{tot}} = & \sum_{\text{bond}} \frac{1}{2} K_r (r - r_{\text{eq}})^2 + \sum_{\text{angle}} \frac{1}{2} K_\theta (\cos \theta - \cos \theta_{\text{eq}})^2 + \sum_{\text{dihedral}} \frac{1}{2} K_\chi [1 - \cos(n\chi - \delta)] \\
 & + \sum_{\text{improper}} \frac{1}{2} K_\phi (\phi - \phi_{\text{eq}})^2 + \sum_{i=1}^{N-1} \sum_{j>i}^N \left[\frac{A_{ij}}{r_{ij}^{12}} - \frac{B_{ij}}{r_{ij}^6} + \frac{q_i q_j}{r_{ij}} \right]
 \end{aligned}
 \tag{1}$$

130 where V_{tot} is the total interaction potential energy of the system. Harmonic potentials govern
 131 bond length, bond angle, and improper angle motion about nominal values, r_{eq} , θ_{eq} , and ϕ_{eq} and
 132 dihedral angles were modeled by Taylor cosine series. The results of DFT optimization,

133 B3LYP/6-311++G(d,p) level of theory, were applied for r_{eq} , θ_{eq} , and ϕ_{eq} , and δ in standard form
134 of molecular mechanics force field. The short range van der Waals interaction was expressed by
135 the typical Lennard-Jones (12-6) function with the parameters for unlike atoms obtained using
136 the Lorentz-Berthelot combining rule. Columbic interactions were modeled using fixed natural
137 bond orbital analysis to compute partial charges on each atom center. Long-range electrostatic
138 interactions were accounted by using Ewald procedure³⁴⁻³⁸ within the isothermal-isobaric (*NPT*)
139 ensemble at 3 temperature values, 298.15 K, 308.15 K, and 318.15 K. Moreover, columbic
140 interactions were modeled using fixed partial charges on each atom center obtained by natural
141 bond orbital, NBO, analysis and force constants including K_r , K_θ , K_χ , K_ϕ , besides the
142 intermolecular Lennard-Jones (12-6) parameters, A and B , were taken from Mayo et al.³³ study.
143 A cubic box containing 512 molecules with a period of 1 ns *NPT* (constant number of particles,
144 constant pressure, and constant temperature) ensemble simulation was performed to adjust the
145 simulation system achieving proper density at pressure of 1.01325 bar. The time step was set to
146 be 1 fs and the equilibrium process was preset to 700 ps. After reaching equilibrium state, the
147 system keeps running for 300 ps to collect the required data with the applied force field.

148 Neighborhood lists were updated every 10 time steps with a distance of 15 Å. Full
149 electrostatic evaluations were calculated. The coupling methods for pressure and temperature
150 were applied by Nose-hoover thermostat-barostat every 1.0 and 0.1 ps, respectively.^{36,37} Using
151 Verlet leapfrog scheme,³⁸ the positions and velocities of particles were calculated.

152 The external magnetic field aligned along the Z direction at different temperatures may shed
153 light on the thermodynamic, transport, and structural properties of the solvent using MD
154 computation. All MD simulations were conducted using DL_POLY version 2.17 simulation
155 package.^{39,40} Notice that all mentioned details of simulation were applied in the case that the

156 complex is present; mole fraction of the complex is 0.002 and the effect of temperature and
157 magnetic field was studied. In this case, the cut off distance was set to 16 Å.

158 In this study, a static and constant magnetic field parallel to the Z-direction of the simulation
159 box was applied. According to the Lorentz force, the output of the magnetic field depends on the
160 velocity of solvent flow, magnetic force, number of particles with positive or negative charges in
161 solvent, and the angle between particle velocity and applied magnetic field, which is always
162 upright.

163 An accurate practical means for the analysis of the structure is provided by pair correlation
164 function, $g(r)$, defined as:

$$165 \quad g(r) = \rho^{-2} \left\langle \sum_i \sum_{i \neq j} \delta(r_i) \delta(r_j - r) \right\rangle \quad (2)$$

166 with r is the atomic separation and ρ the number density; r_i and r_j are the atomic positions.
167 Atom-atom pair correlation functions made available from the histogram of trajectories were
168 applied to estimate the spreading profile and thus the structural relation between the solvent
169 atoms. In addition, the coordination numbers were computed by the aid of the RDF. The
170 coordination number of the solvation is deduced from the solvent-solute pair correlation
171 functions. The integral over the pair correlation function reveals the number of neighbors as
172 function of their distance

$$173 \quad N(r) = 4\pi\rho \int_0^r g(r)r^2 dr \quad (3)$$

174 Here ρ represents the number density of the selected atom species. Integration over the entire
175 first peak leads to a consistent number of nearest neighbors.

176 Besides, the molecular mobility was investigated by mean-square displacement.

$$177 \quad MSD = \left\langle \left| r_j(t) - r_j(0) \right|^2 \right\rangle \quad (4)$$

178

179

180 **Results and discussion**181 *Conductance studies*

182 The changes of molar conductivity (Λ_m) versus the ligand to the metal cation mole ratio,
183 ($[L]_t/[M]_t$), for complexation of kryptofix 22DD with La^{3+} cation in ordinary and magnetized
184 methanol solvents were studied at different temperatures. The resulting molar conductivity
185 versus $[L]_t/[M]_t$ in these two conditions are shown in Figures 1 and 2. As it is evident in these
186 figures, addition of kryptofix 22DD to La^{3+} cation solution results in an increase in molar
187 conductivity which indicates that the $(\text{kryptofix 22DD}.\text{La})^{3+}$ complex is in considerable amount
188 than the free solvated La^{3+} cation. This result may be explained on the basis of the solvation
189 sphere. It seems that La^{3+} cation is solvated to a high extent in this organic solvent. Upon
190 complexation of the metal cation with kryptofix 22DD, the ligand molecule replaces the
191 solvation sheath around the metal ion and the resulting complex becomes less bulky; therefore,
192 the molar conductivity increases by ligand addition to the cation solution.

193 As is shown in Figure 1, the slope of the corresponding molar conductivity versus $[L]_t/[M]_t$
194 changes at the point where the ligand to cation mole ratio is about one which is an evidence for
195 formation of a relatively stable 1:1[M:L] complex between kryptofix 22DD and La^{3+} cation in
196 ordinary methanol solvent. On the other hand, the plot of corresponding molar conductivity
197 versus $[L]_t/[M]_t$ does not show any considerable change in slope emphasizing the formation of
198 relatively weak 1:1[M:L] complex in the magnetized methanol solvent (see Figure 2).

199

200

< Figure 1 and 2 >

201

202 In order to make the 1:1[M:L] complex model more clear, the fitting and the experimental
203 curves for the (kryptofix 22DD.La)³⁺ complex in magnetized methanol solvent at 298.15 K is
204 shown in Figure 3. As it is clearly evident in this Figure, there is an accurate acceptable
205 agreement between experimental and least square regression.

206

207

< Figure 3 >

208

209 To gather accurate information about the conformational change of kryptofix 22DD upon
210 complexation with lanthanum (III) cation, the molecular structures of the uncomplexed ligand
211 and its 1:1 La³⁺ complex were computed with quantum calculations. The structure of the free
212 ligand was optimized at B3LYP/Lan12dz level of theory. The optimized structure of the ligand
213 was then applied to find out the initial structure of its 1:1 lanthanum (III) complex (at the same
214 level of theory). The optimized structures of the uncomplexed ligand (i.e. kryptofix 22DD) and
215 its 1:1 complex with La³⁺ cation (i.e. kryptofix 22DD.La)³⁺ are presented in Figure 4. In order to
216 study the effect of solvent upon complexation, we compared the order of stability of the
217 complexes formed between kryptofix 22DD and La³⁺ cation in the gas phase which were
218 obtained based on binding energies with the order of stability of the complexes formed between
219 kryptofix 22DD and La³⁺ cation in the presence of methanol. Figure 4A and 4B show the
220 optimized structures of free ligand and its complex with La³⁺ cation in the gas phase. It is
221 obvious from Figure 4A that the ligand forms a more or less planar but interestingly, in the
222 optimized structure of the 1:1 (kryptofix 22DD.La)³⁺ complex (Figure 4B), lanthanum (III) ion is
223 well incorporated inside the twisted macrocyclic ligand and coordinated to six donating atoms of

224 the ligand, including four oxygen atoms and two nitrogen. It is fascinating to note that when the
225 metal ion is added to the ligand, the ligand was twisted and completely deformed from its planar
226 shape. Moreover, the orientation of two carbon chains attached to the ring changes in comparison
227 with the free ligand. The optimized structures of free ligand and its complex with La^{3+} in the
228 presence of methanol were also studied. For the calculations in the presence of methanol as a
229 solvent, the Polarizable Continuum Model (PCM) was chosen. In this model, the cavity is
230 created via a series of overlapping spheres. The PCM was applied within the B3LYP/LanL2DZ
231 level to predict the solvent effects on the structures and interaction energy of kryptofix 22DD
232 ligand and $[\text{kryptofix 22DD.La}]^{3+}$. The results show, there is no major changes occurred in the
233 structures of free ligand and its complex in comparison to the gas phase calculation. For this
234 reason, the structures of free ligand and its complex are not shown in the presence of methanol.
235 Moreover, the effect of solvent on the binding energy of complex was investigated. The pair
236 wise binding energy ΔE between kryptofix 22DD ligand and La^{3+} is estimated as the difference
237 between the energy of the complex $[\text{kryptofix 22DD.La}]^{3+}$ and the energies of isolated partners:

$$238 \quad \Delta E = E_{[\text{kryptofix 22DD.La}]^{3+}} - (E_{\text{La}^{3+}} + E_{\text{kryptofix 22DD}})$$

239 The binding energy for the $[\text{kryptofix 22DD.La}]^{3+}$ complex were obtained -53.1 and - 481.2
240 kcal. mol^{-1} in the gas phase and in the presence of methanol, respectively. This results show that
241 the stable complex is formed in the presence of methanol as a solvent.

242

243

< Figure 4 >

244

245 Now, the question is how the magnetic field impacts on the solvent and how this magnetized
246 solvent can change the thermodynamic of the complexation process between the kryptofix 22DD

247 and La^{3+} cation. Chang and Weng¹⁷ have investigated the effects of the magnetic field on the
248 hydrogen-bonded structure of water and they found that the number of the hydrogen bonds
249 increases when it is exposed to a magnetic field. Since water molecules have two donors and two
250 acceptor sites, liquid water forms a continuous network of hydrogen bonds. The presence of
251 spatial network of hydrogen bonds is the main property of the liquid water.⁴¹ Furthermore, some
252 researchers have carried out a series of studies to know if there is any relationship between the
253 hydrogen bonding and temperature of water.^{42,43} It has been recognized that the hydrogen
254 bonding becomes weaker with increasing the thermal motion of the atoms involved.⁴⁴
255 Consequently, the water structure breaks down as the temperature increases. It has been
256 suggested that the effects of a magnetic field on water hydrogen bonds are similar with the
257 effects of decreasing the temperature.⁴⁵ The theory of cluster models points out that the average
258 size of water cluster decreases with increasing temperature.^{46,47} Normally, the viscosity and also
259 the dielectric constant of liquid water decreases as the temperature increases.^{48,49} From the other
260 side of view, methanol is a polar solvent and its molecules are able to constitute hydrogen bonds
261 through their hydrogen and oxygen atoms; therefore, it is expected a similar behavior is observed
262 for this organic solvent as water. It has been shown that the hydrogen bond network in methanol
263 molecules increases as the temperature decreases.⁵⁰ In addition, the viscosity and the dielectric
264 constant of the liquid methanol increase as the temperature decreases.^{49,51}

265 The values of the stability constant ($\log K_f$) of (kryptofix 22DD.La)³⁺ complex are given in
266 Table 1. It can be seen that by applying magnetic field, the stability of the (kryptofix 22DD.La)³⁺
267 complex decreases at all studied temperatures. Similar results have been observed by the authors
268 in the previous study which further corroborate the results reported in Table 1.⁵² This result may
269 be attributed to the higher dielectric constant and possibly changing the donor number of the

270 magnetized methanol solvent than that of the ordinary methanol. The higher dielectric constant
271 and change in the donicity of the magnetized solvent with respect to the ordinary methanol may
272 lessen the electrostatic interactions between the ligand and La^{3+} cation. As a result, the complex
273 formation between kryptofix and La^{3+} cation weakens by imposing magnetic field on the solvent.
274 Furthermore, it seems that the higher viscosity of the magnetized methanol solvent, leads to a
275 decrease in the rate of the complexation reaction in this extraordinary solvent compared to the
276 ordinary methanol solvent.

277

278

< Table 1 >

279

280 In order to shed light on this suggestion, MD was handled and the results are given in the
281 following paragraphs.

282 *Molecular dynamics studies*

283 As mentioned before, the formation of hydrogen bonding between the methanol solvent
284 molecules enhances due to the external magnetic field and its temperature effect is one of the
285 substantial questions that are under study in the present research work. Figure 5 compares the
286 variation of hydrogen bond, O–H distance, in the present solvent at three different temperatures
287 in the presence and absence of magnetic field. As evidence from this figure, external magnetic
288 field has a direct effect on the structure of the solvent; in other words, the molecules are more
289 ordered and stable. To evaluate the average number of hydrogen bonds, the present study adopts
290 the geometric criterion⁵³ that a hydrogen bond will be formed if the distance between the oxygen
291 and hydrogen atoms of a pair of methanol molecule is less than the first minimum of the O–H
292 radial distribution function, 2.52 Å. This procedure has been applied on water molecules by

293 Levitt et al.⁵⁴ The simulation results presented in Figure 5 indicate that applying magnetic field
294 intensifies the strength of hydrogen bond. Besides, as the temperature increases from 298.15 K to
295 318.15 K, the average variation of O–H bond length increases. The slight increase in the O–H
296 bond length with increasing the temperature demonstrates the magnetic field enhances the
297 networking ability and the temperature has an opposite effect. Moreover, near connection
298 between H and O atoms of the methanol molecules implies that the cluster size increases under a
299 magnetic field, and hence more compact in the structure of methanol molecules is observed. The
300 results of this study show that the number of hydrogen bonds between the methanol molecules
301 increases which are consistent with the findings reported before²⁰ and it has been suggested that
302 the enhancement of the hydrogen bond strength under an external magnetic field is caused by the
303 increasing the electron delocalization of the hydrogen bonded molecules. Furthermore, the effect
304 of the magnetic field in increasing the number of hydrogen bonds is consistent with the
305 weakening van der Waals bonding force between the solvent molecules under a magnetic field²⁵
306 and the suppression of thermal motions because of the tighter hydrogen bonding induced by the
307 Lorentz forces.²¹

308

309 < Figure 5 >

310

311 Commonly, radial distribution function (RDF) examines the structure of a liquid; in the case
312 of methanol, gO–H and gO–O are considered to investigate the structural dependence on the
313 external magnetic field. The other correlations as C–C, C–H, and H–H show insignificant
314 revolution with magnetic field that are not shown. In other words, the correlations due to
315 hydrogen bond enjoy considerable variations that are under study here. The structural differences

316 of pure liquid with and without the application of an external magnetic field are depicted for gO–
317 H in Figure 6, at T=298.15, 308.15, and 318.15 K. The first peak occurs at 2.575 Å, at the
318 absence of the magnetic field and at T=298.15 K, which corresponds to the oxygen-hydrogen
319 distance between the two hydrogen-bonding methanol molecules, which reduces to 2.525 Å, at
320 T=298.15 K and the presence of the magnetic field. It should be noted that this distance is greater
321 than an O–H bond length obtained by DFT computation (0.961 Å), i.e., the aforementioned
322 distance does not correspond to the O–H bond length. The tetrahedral structure of the near
323 neighbors is related to the second peak of O–H RDF belonging to two molecules both hydrogen
324 bonded to a third methanol.

325

326

< Figure 6 >

327

328 In order to shed light on the compactness of methanol molecules because of magnetic field,
329 O–O RDF, the distribution of the oxygen atoms of the methanol molecules, at T=298.15 K,
330 308.15 K, and 318.15 K was also considered, Figure 7. Surprisingly, the distance between two
331 methanol molecules in the absence and presence of the magnetic field is unchanged (3.475 Å)
332 and the intensity of the peak just only increases sharply. However, the height of the second peak
333 shows a slight change indicating the distance between the two oxygen atoms of two next-nearest
334 neighbors is not influenced by the magnetic field. From the other side of view, the average
335 tetrahedral hydrogen bonding length may not be affected by external magnetic field. The
336 increased height of the first and second valleys under external magnetic field demonstrates that
337 more molecules exist between methanol shells. The slight increase in the height of the first valley
338 indicates that more molecules are located between the shells. However, magnetic field reforms

339 the structure of the liquid methanol, forces more methanol molecules between the shells, and
340 enhances the connectivity between molecules to progress the stability of the solvent-solvent
341 network. Consequently, a small increase in the number of hydrogen bonds is apparent under an
342 external magnetic field. According to the results presented in Figure 7, the methanol molecules
343 tend to form more stable connections with other molecules in all directions.

344

345 < Figure 7 >

346

347 In summary, the results presented in Figures 6 and 7 demonstrate that the magnetic field
348 enhances the binding between the methanol molecules and stabilize the structure of the liquid
349 methanol.

350 In this study, we also investigated the self-diffusion coefficients of the solvent molecules
351 under a magnetic field. Study of the transport properties of a liquid is an important topic, both in
352 fundamental sciences and also in its applications. The mobility of methanol molecules is
353 indicated by the value of mean-square displacement (MSD), which depends on the temperature,
354 pressure, structure, and so on. The value of the self-diffusion coefficients can be obtained from
355 the Einstein relation based on MSD function. The present results show that a static magnetic
356 field enhances the stability of methanol molecules and hence influences their mobility.
357 Calculating the self-diffusion coefficient of the molecules provides a clearer understanding of
358 their change in mobility. Figure 8 presents the profiles of MSD under various temperatures and
359 magnetic strengths. It is noticeable that the self-diffusion coefficient reduces as the magnetic
360 field is applied. The decreasing self-diffusion coefficient by applying magnetic field points to the
361 mobility decrease of methanol molecules. If the molecule mobility changes, the physical

362 properties such as viscosity, thermal conductivity, and their melting point also change. Although
363 the decrease of the self-diffusion coefficient caused by the magnetic field is not large, it indicates
364 a change in the properties of the liquid. In general, based on the above finding, it seems that the
365 changes of structure of the methanol solvent under the influence of the magnetic field are
366 probably effective in changing the (kryptofix 22DD.Y)³⁺ complex stabilization in solution.

367

368 < Figure 8 >

369

370 Now it is the point to emphasize on the second target of this computation. The goal is to
371 investigate the effect of magnetic field on the complex stabilization since a molecular knowledge
372 about the solvent and magnetic field is present. For this aim, a system containing the complex
373 and solvent was simulated. The results of atomic RDF between the solvent, hydrogen atom
374 connected to oxygen atom of complex represented by H(O), and the complex, N atom, at the
375 presence of magnetic field and its absence are presented in Figure 9. As the figure demonstrates,
376 the complex interaction with the solvent increases at a distance about 3 Å with magnetic field
377 without any substantial variation of distance between solvent and complex. Interestingly, the
378 complex structure does not witness change showing that the complex is stable at the presence of
379 magnetic field. However, the observation was quantified by computing coordination number
380 where at different temperatures is compared between the system at the presence of magnetic field
381 and its absence in Table 2. As the table tabulates, the previous statement is confirmed by
382 coordination number values.

383

384 < Figure 9 >

385 < Table 2 >

386

387 Based on Table 2, it can be understood that coordination number (CN) of methanol at the
388 presence of magnetic field enhances that is in good agreement with the decreasing temperature.
389 However, the complex presence leads to a very slight decrease of coordination number.
390 Additionally, the intermolecular interaction between the complex and the solvent may lessens the
391 magnetic field effect on the solvent; as a result, the CN is less than its corresponding value for
392 the pure methanol and the presence of magnetic field. In other words, the strong interaction
393 between complex and solvent at magnetic field causes retard of complex provide.

394 **Conclusions**

395 Actually, in the host-guest recognition processes, the solvent plays a critical role in the local
396 structure optimization and complex stabilization; thus, the stability of the metal ion complexes is
397 known to vary drastically according to the chemical and physical properties of the solvent in
398 which the complexation reactions occur. In the present work, we investigated the effect of
399 methanol solvent properties on complexation reaction of the kryptofix 22DD with La^{3+} cation.
400 The values of the stability constant of $(\text{kryptofix 22DD.La})^{3+}$ complex in both ordinary and
401 magnetized methanol solvent were determined by electrical conductance measurements. The
402 results show that the stability constants of the complex at different temperatures in magnetized
403 methanol solution are lower than those obtained in the case of ordinary methanol. It seems that
404 the changes of structure, viscosity, and the dielectric constant of the studied organic solvent
405 under the influence of magnetic field are probably effective in changing the $(\text{kryptofix}$
406 $22\text{DD.La})^{3+}$ complex stabilization.

407 In addition, molecular dynamics simulation was applied to examine the effect of a static
408 magnetic field on the liquid methanol at a various temperatures of 298.15, 308.15, and 318.15 K.
409 It has been shown that an external magnetic field influences the number of hydrogen bonds, its
410 strength, the structure of the liquid methanol, as well as its molecular mobility. The increasing
411 number of the hydrogen bonds, due to the external magnetic field, indicates the formation of
412 larger methanol molecule clusters. The magnetic field induces a tighter bonding between the
413 methanol molecules and improves the stability of this liquid. Under the effect of the magnetic
414 field, the structure of the liquid changes and more molecules are forced between the methanol
415 shells decreasing the stability of the complex.

416 These molecules connect the shells and hence create a more stable methanol-methanol
417 network. The transport properties of the molecules, as indicated by MSD, are of considerable
418 interest in many applications. The current simulation results have shown that the molecular
419 mobility reduces when a magnetic field is applied to the methanol solvent and, hence, resulting
420 in a reduction in the self-diffusion coefficient of this organic solvent. In other words, the
421 magnetic field constrains the movement of the methanol molecules, and hence changes both the
422 thermal conduction and the viscosity in the liquid state. This change is in a good agreement with
423 decreasing the stability constant of the (kryptofix 22DD.La)³⁺ complex in magnetized methanol
424 compared to the ordinary methanol solvent.

425

426 **Acknowledgements**

427 The authors wish to acknowledge the financial supports (No. 18232) of this work by Ferdowsi
428 University of Mashhad, Mashhad, Iran.

429

430 **References**

- 431 1 R.Z. Gnann, R.I. Wagner, K.O. Christe, R. Bau, G.A. Olah and W.W. Wilson, *J. Am. Chem.*
432 *Soc.*, 1997, **119**, 112–115.
- 433 2 P. Ghosh, P.K. Bharadwaj, J. Roy and S. Ghosh, *J. Am. Chem. Soc.*, 1997, **119**, 11903–11909.
- 434 3 P. Chang and J.S. Shih, *Anal. Chim. Acta*, 1999, **380**, 55–62.
- 435 4 R. Cacciapaglia, L. Mandolini and V.V.A. Castelli, *J. Org. Chem.*, 1997, **62**, 3089–3092.
- 436 5 M.J. Wagner, A.S. Ichimura, R.H. Huang, R.C. Phillips and J.L. Dye, *J. Phys. Chem. B*, 2000,
437 **104**, 1078–1087.
- 438 6 B. Dietrich, J.M. Lehn and J.P. Sauvage, *Tetrahedron Lett.*, 1969, **10**, 2885–2888.
- 439 7 J.M. Lehn, *Pure Appl. Chem.*, 1978, **50**, 871–892.
- 440 8 R.M. Izatt, K. Pawlak, J.S. Bradshaw and R.L. Bruening, *Chem. Rev.*, 1991, **91**, 1721–2085.
- 441 9 J.M. Lehn and J.P. Sauvage, *J. Am. Chem. Soc.*, 1975, **97**, 6700–6707.
- 442 10 R.E. Kirk and D.F. Othmer, *Encyclopedia of Chemical Technology*. Wiley, 1982, **19**, 836.
- 443 11 C.-B. Liu, C.-Y. Sun, L.-P. Jin and S.-Z. Lu, *New J. Chem.*, 2004, **28**, 1019–1026.
- 444 12 C.-B. Liu, M.-X. Yu, X.-J. Zheng, L.-P. Jin, S. Gao and S.-Z. Lu, *Inorg. Chim. Acta*, 2005,
445 **358**, 2687–2696.
- 446 13 X.-J. Zheng, L.-P. Jin and S. Gao, *Inorg. Chem.*, 2004, **43**, 1600–1602.
- 447 14 M. Watanabe, T. Nankawa, T. Yamada, T. Kimura, K. Namiki, M. Murata, H. Nishihara and
448 S. Tachimori, *Inorg. Chem.*, 2003, **42**, 6977–6979.
- 449 15 V. Patroniak, P.N.W. Baxter, J.-M. Lehn, Z. Hnatejko and M. Kubicki, *Eur. J. Inorg. Chem.*,
450 2004, 2379–2384.
- 451 16 R.G. Cooks and T.L. Kruger, *J. Am. Chem. Soc.*, 1977, **99**, 1279–1281.
- 452 17 N. Verdel and Peter Bukovec, *Entropy*, 2014, **16**, 2146–2160.
- 453 18 S.-H. Lee, M. Takeda and K. Nishigaki, *Jpn. J. Appl. Phys.*, 2003, **42**, 1828–1833
- 454 19 M. Iwasaka and S. Ueno, *J. Appl. Phys.*, 1998, **83**, 6459–6461.
- 455 20 H. Hosoda, H. Mori, N. Sogoshi, A. Nagasawa and S. Nakabayashi, *J. Phys. Chem. A*, 2004,
456 **108**, 1461–1464.
- 457 21 H. Inaba, T. Saitou, K.-i. Tozaki and H. Hayashi, *J. Appl. Phys.*, 2004, **96**, 6127–6132.
- 458 22 S. Hakobyan and S. Ayrapetyan, *Biofizika*, 2005, **50**, 265–270.
- 459 23 T. Itoi and A. Inoue, *Mater. Trans.*, 2000, **41**, 1256–1262.
- 460 24 A. Sugiyama, S. Morisaki and R. Aogaki, *Mater. Trans.*, 2000, **41**, 1019–1025.

- 461 25 R.V. Krems, *Phys. Rev. Lett.*, 2004, **93**, 013201–4
- 462 26 M. Einax, W. Dieterich and P. Maass, *Rev. Mod. Phys.*, 2013, **85**, 921–939.
- 463 27 M. Einax, S. Heinrichs, P. Maass, A. Majhofer and W. Dieterich, *J. Phys. Condens. Matter*,
464 2007, **19**, 086227.
- 465 28 Genplot, *A data analysis and graphical plotting program for scientist and engineers*.
466 *computer graphic service*, Ltd., Ithaca, New York, 1989.
- 467 29 Y. Yang, T.A. Pakkanen and R.L. Rowley, *Int. J. Thermophys.*, 2000, **21**, 703–717.
- 468 30 X. Li, M.D. Sevilla and L. Sanche, *J. Am. Chem. Soc.*, 2003, **125**, 8916–8920.
- 469 31 A. Dkhissi, L. Houben, J. Smets, L. Adamowicz and G. Maes, *J. Phys. Chem. A*, 2000, **104**,
470 9785–9792.
- 471 32 M.J. Frisch, G.W. Trucks, H.B. Schlegel, G.E. Scuseria, M.A. Robb, J.R. Cheeseman, J.A.
472 Montgomery, T. Vreven, K.N. Kudin, J.C. Burant, J.M. Millam, S.S. Iyengar, J. Tomasi, V.
473 Barone, B. Mennucci, M. Cossi, G. Scalmani, N. Rega, G.A. Petersson, H. Nakatsuji, M. Hada,
474 M. Ehara, K. Toyota, R. Fukuda, J. Hasegawa, M. Ishida, T. Nakajima, Y. Honda, O. Kitao, H.
475 Nakai, M. Klene, X. Li, J.E. Knox, H.P. Hratchian, J.B. Cross, V. Bakken, C. Adamo, J.
476 Jaramillo, R. Gomperts, R.E. Stratmann, O. Yazyev, A.J. Austin, R. Cammi, C. Pomelli, J.W.
477 Ochterski, P.Y. Ayala, K. Morokuma, G.A. Voth, P. Salvador, J.J. Dannenberg, V.G.
478 Zakrzewski, S. Dapprich, A.D. Daniels, M.C. Strain, O. Farkas, D.K. Malick, A.D. Rabuck, K.
479 Raghavachari, J.B. Foresman, J.V. Ortiz, Q. Cui, A.G. Baboul, S. Clifford, J. Cioslowski, B.B.
480 Stefanov, G. Liu, A. Liashenko, P. Piskorz, I. Komaromi, R.L. Martin, D.J. Fox, T. Keith, A.
481 Laham, C.Y. Peng, A. Nanayakkara, M. Challacombe, P.M.W. Gill, B. Johnson, W. Chen, M.W.
482 Wong, C. Gonzalez and J.A. Pople, *Gaussian 03*, Revision C.02.
- 483 33 S.L. Mayo, B.D. Olafson and W.A. Goddard, *J. Phys. Chem.*, 1990, **94**, 8897–8909.
- 484 34 M. Kohagen, M. Brehm, J. Thar, W. Zhao, F. Müller-Plathe and B. Kirchner, *J. Phys. Chem.*
485 *B*, 2010, **115**, 693–702.
- 486 35 O. Guvench, S.N. Greene, G. Kamath, J.W. Brady, R.M. Venable, R.W. Pastor and A.D.
487 Mackerell, *J. Comput. Chem.*, 2008, **29**, 2543–2564.
- 488 36 L. Weng, C. Chen, J. Zuo and W. Li, *J. Phys. Chem. A*, 2011, **115**, 4729–4737.
- 489 37 C. Chen, W.Z. Li, Y.C. Song and J. Yang, *J. Mol. Liq.*, 2009, **146**, 23–28.

- 490 38 M.P. Allen and D.J. Tildesley, *Computer simulation of liquids*. Oxford University Press,
491 1989.
- 492 39 W. Smith and T.R. Forester, *J. Mol. Graphics*, 1996, **14**, 136–141.
- 493 40 T. Forester and W. Smith, *The DL_POLY_2 Reference Manual*, Daresbury Laboratory,
494 Daresbury, 2000.
- 495 41 N.A. Chumaevskii and M.N. Rodnikova, *J. Mol. Liq.*, 2003, **106**, 167–177
- 496 42 R. Li, Z. Jiang, H. Yang and Y. Guan, *J. Mol. Liq.*, 2006, **126**, 14–18.
- 497 43 J. Urquidi, C.H. Cho, S. Singh and G.W. Robinson, *J. Mol. Struct.*, 1999, **485**, 363–371.
- 498 44 G.A. Jeffrey, *An Introduction to Hydrogen Bonding*, Oxford University Press, 1997.
- 499 45 R. Cai, H. Yang, J. He and W. Zhu, *J. Mol. Struct.*, 2009, **938**, 15–19.
- 500 46 M. Starzak and M. Mathlouthi, *Food Chem.*, 2003, **82**, 3–22.
- 501 47 A.T. Hagler, H.A. Scheraga and G. Némethy, *J. Phys. Chem.*, 1972, **76**, 3229–3243.
- 502 48 F. Franks, *Water: a comprehensive treatise*, Plenum Press, New York, 1972–1980.
- 503 49 M. Mohsen-Nia, H. Amiri and B. Jazi, *J. Solution Chem.*, 2010, **39**, 701–708.
- 504 50 S.L. Wallen, B.J. Palmer, B.C. Garrett and C.R. Yonker, *J. Phys. Chem.*, 1996, **100**, 3959–
505 3964.
- 506 51 A.M. Katti, N.E. Tarfulea, C.J. Hopper and K.R. Kmiotek, *J. Chem. Eng. Data.*, 2008, **53**,
507 2865–2872.
- 508 52 M. Gholizadeh, G. H. Rounaghi, I. Razavipanah and M. R. Salavati, *J. Iran Chem. Soc.*, 2014, **11**,
509 947–952.
- 510 53 I. Benjamin, *J. Chem. Phys.*, 1992, **97**, 1432–1445.
- 511 54 M. Levitt, M. Hirshberg, R. Sharon, K.E. Laidig and V. Daggett, *J. Phys. Chem. B*, 1997,
512 **101**, 5051–5061.
- 513

514 **Figure captions:**

515 **Figure 1.** Molar conductance-mole ratio plots for (kryptofix 22DD.La)³⁺ complex in methanol
516 solution at different temperatures: 25 °C (open circle), 35 °C (asterisk), 45 °C (open triangle).

517 **Figure 2.** Molar conductance-mole ratio plots for (kryptofix 22DD.La)³⁺ complex in methanol
518 which is exposed to the magnetic field for two minutes at different temperatures: 25 °C (open
519 circle), 35 °C (asterisk), 45 °C (open triangle).

520 **Figure 3.** The experimental data and fitting curve for (kryptofix 22DD.La)³⁺ complex in
521 magnetic methanolic solution at 298.15 K.

522 **Figure 4.** Optimized structures of free kryptofix 22DD (A) and its 1:1 complex with La³⁺ cation
523 (B).

524 **Figure 5.** Comparison of the target solvent H-O distance in the presence and absence of
525 magnetic field at different temperatures.

526 **Figure 6.** Comparison of g(r) O-H in the presence and absence of the magnetic field at different
527 temperatures.

528 **Figure 7.** Comparison of g(r) O-O in the presence and absence of the magnetic field at different
529 temperatures.

530 **Figure 8.** Comparison of the mean-square displacement of the solvent in the presence and
531 absence of the magnetic field at different temperatures.

532 **Figure 9.** Comparison of g(r) N...H(O) in the presence and absence of the magnetic field at
533 different temperatures. The inset is g(r) in the absence of magnetic field at three studied
534 temperatures.

535

536

537

538
539
540
541
542
543
544
545
546
547
548
549
550
551
552
553
554
555
556
557
558
559
560
561
562
563
564
565
566
567

Table 1. Log K_f values of (kryptofix 22DD.La)³⁺ complex in the methanol solution and magnetic methanolic solution at different temperatures

Medium (kryptofix 22DD.La) ³⁺	Log $K_f \pm SD^a$		
	25 °C	35 °C	45 °C
Pure MeOH ^b	3.50 ± 0.04	3.39 ± 0.03	3.36 ± 0.02
Pure MeOH ^c	2.76 ± 0.07	2.50 ± 0.10	2.80 ± 0.09

^aSD = standard deviation

^bIn the absence of the magnetic field

^cIn the presence of the magnetic field

568
569
570
571
572
573
574
575
576
577
578
579
580
581
582
583
584
585
586
587
588
589
590
591
592
593
594
595
596
597
598
599

Table 2. Coordination number (CN) value for methanol at present and absence of magnetic field as well as the complex at different temperatures

CN value		298.15 K	308.15 K	318.15 K
Pure methanol	Magnetic field off	0.89	0.86	0.84
	Magnetic field on	1.26	1.25	1.25
Solution	Magnetic field off	0.88	0.86	0.83
	Magnetic field on	1.23	1.22	1.27

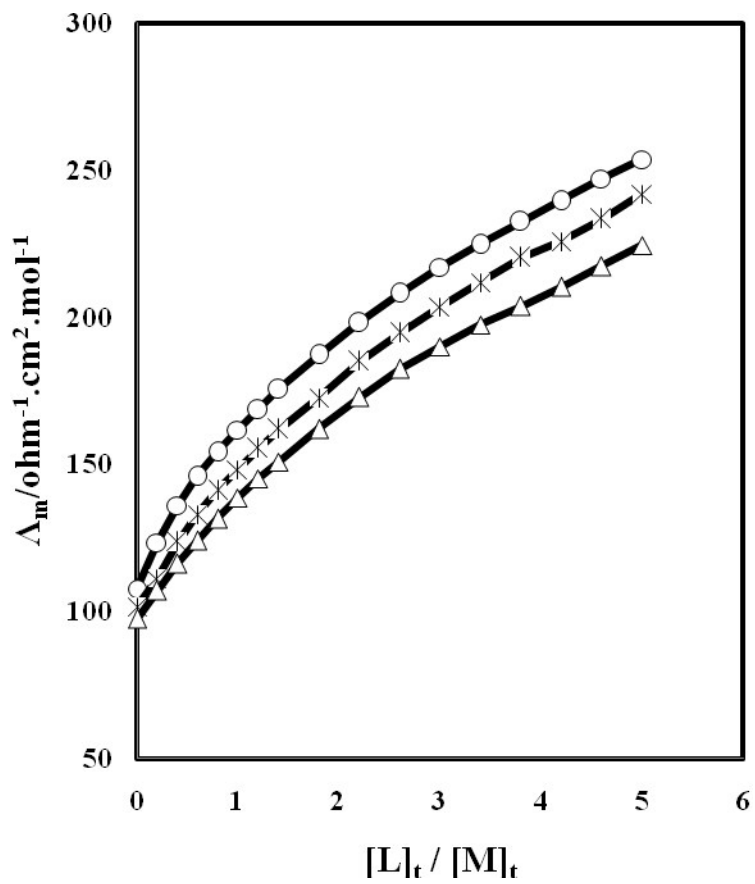


Figure 1

640
641
642
643
644
645
646
647
648
649
650
651
652
653
654
655
656
657
658
659
660
661
662
663
664
665
666
667
668
669
670
671
672
673
674
675
676
677
678
679

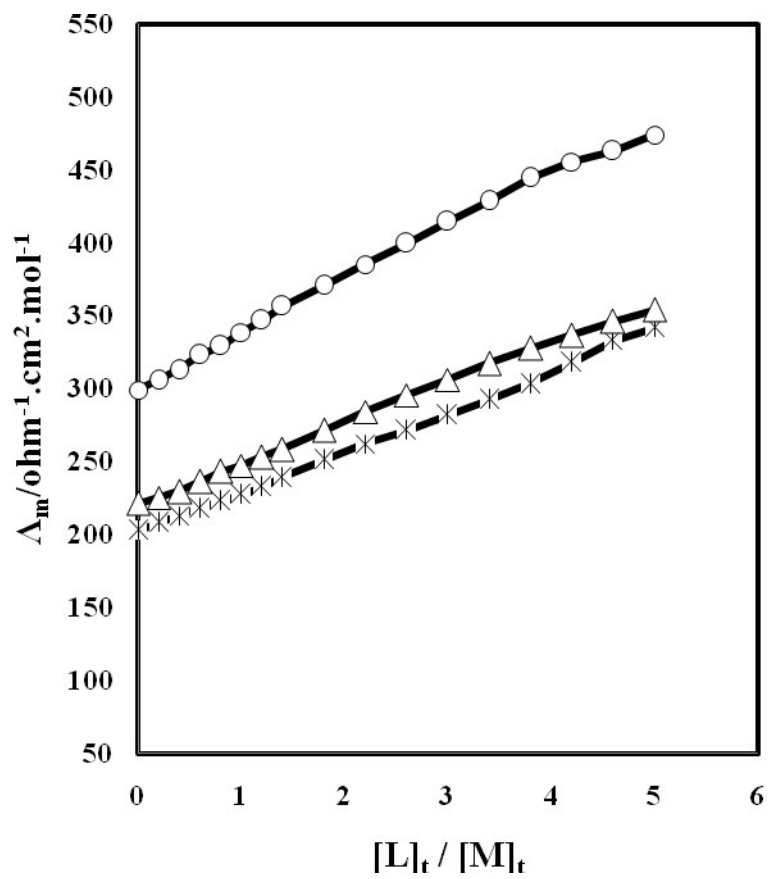
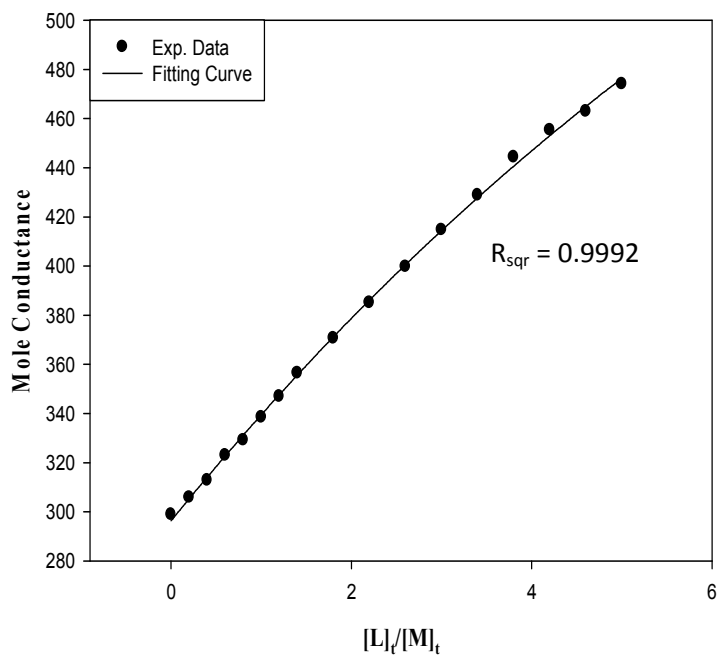


Figure 2

680
681
682
683
684
685
686



687
688
689
690
691
692
693
694
695
696
697
698
699
700
701
702
703

Figure 3

704
705
706
707
708
709
710
711
712
713
714
715
716
717
718
719
720
721
722
723
724
725
726
727
728
729
730
731
732
733
734
735
736
737

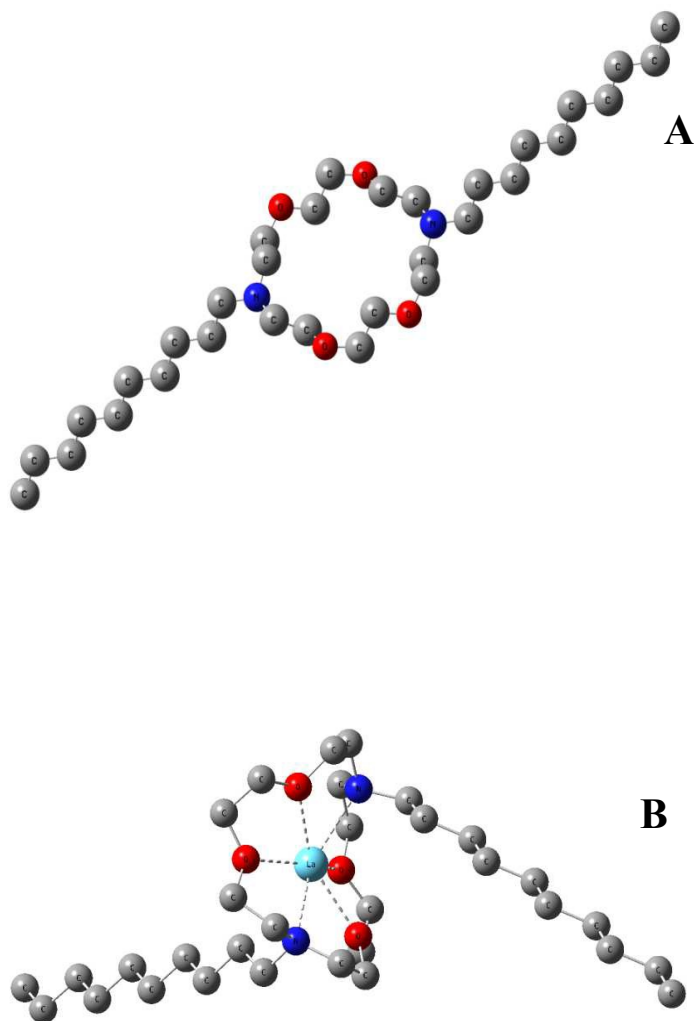
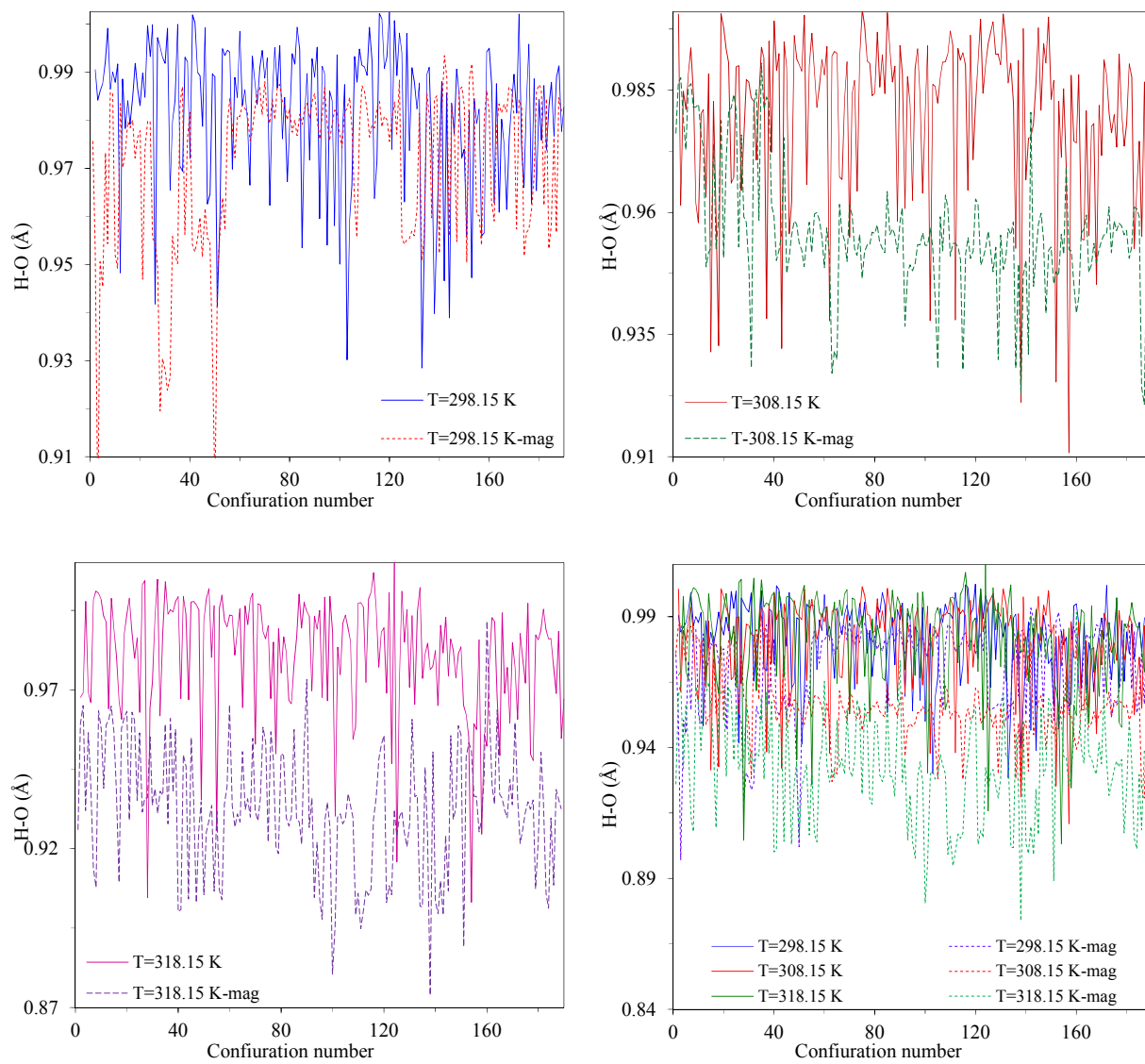


Figure 4



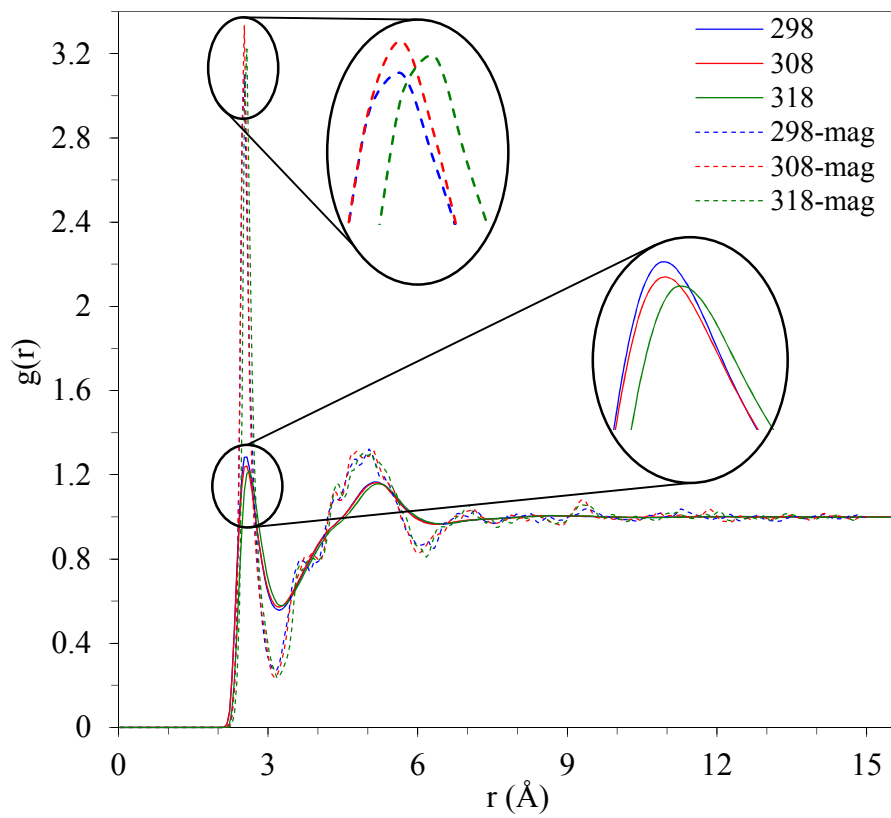
738

739

740

741

Figure 5

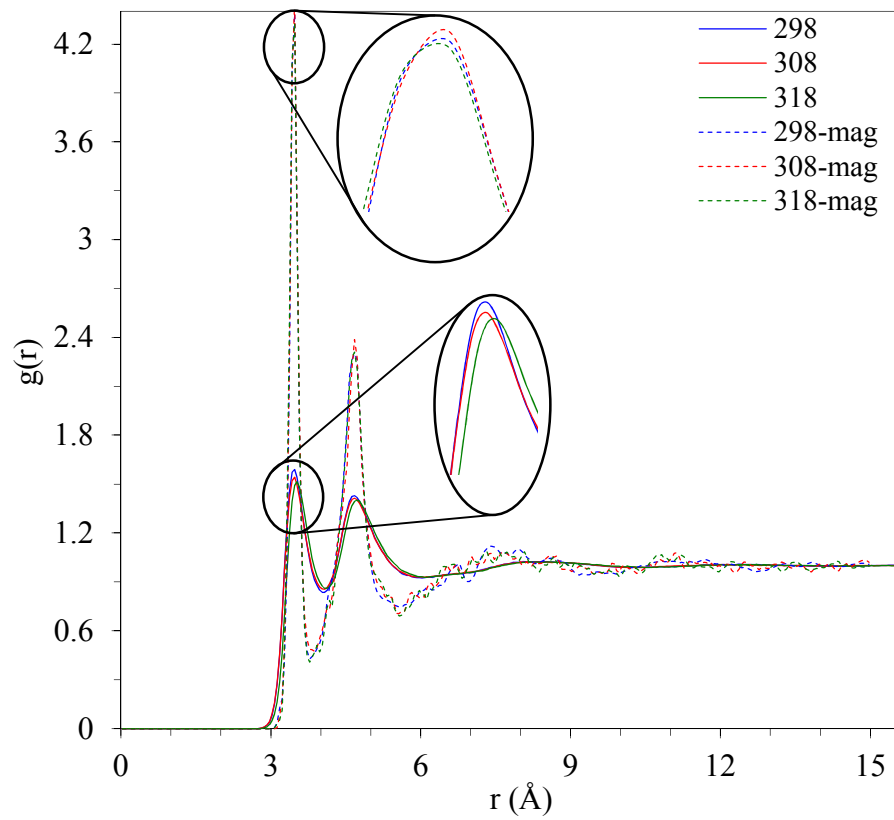


742

743

744

Figure 6

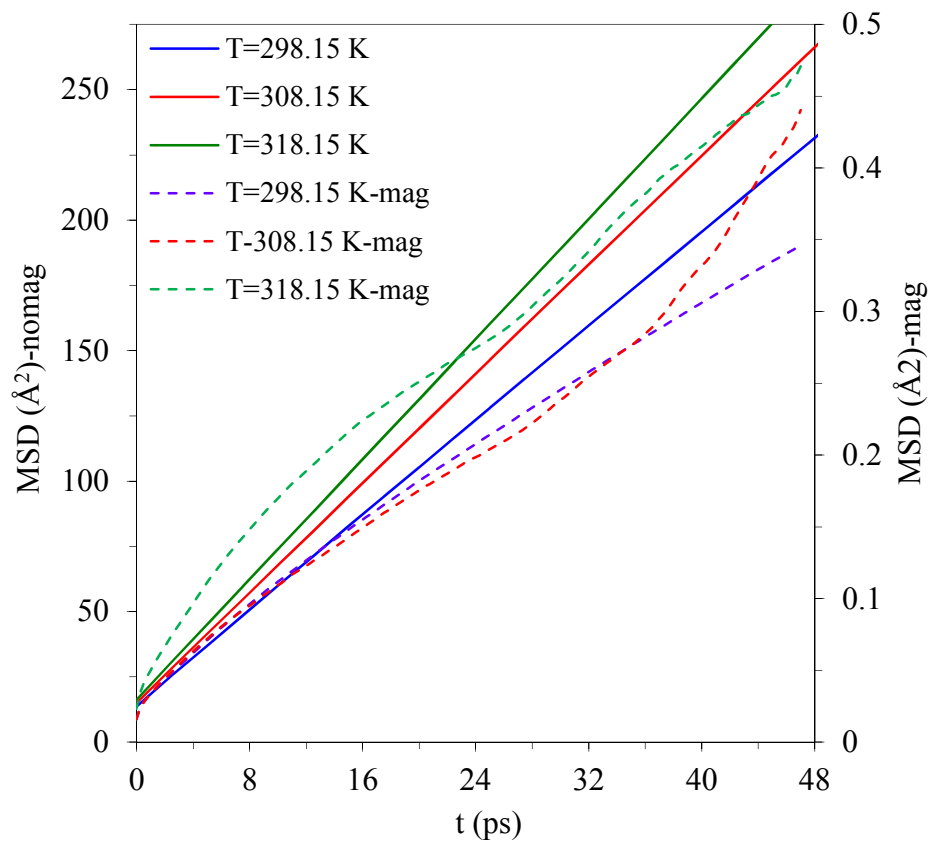


745

746

747

Figure 7

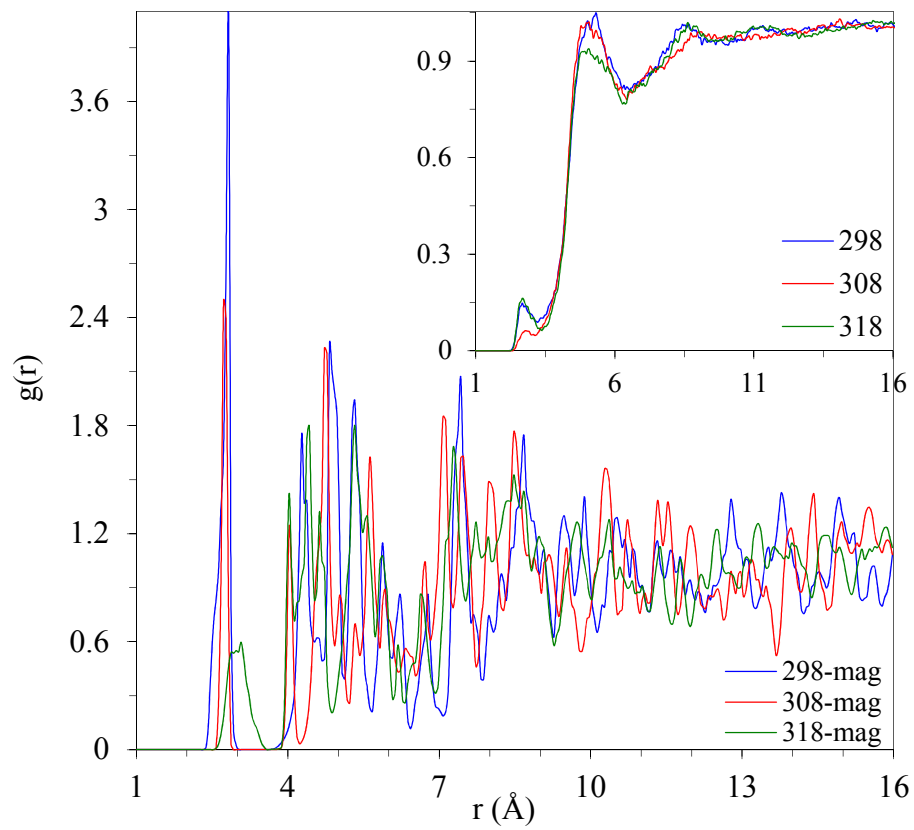


748

749

750

Figure 8



751

752

Figure 9